

A Differential Quadrature Based Approach for Volterra Partial Integro-Differential Equation with a Weakly Singular Kernel

Siraj-ul-Islam¹, Arshed Ali^{2,*}, Aqib Zafar¹ and Iltaf Hussain¹

Abstract: Differential quadrature method is employed by numerous researchers due to its numerical accuracy and computational efficiency, and is mentioned as potential alternative of conventional numerical methods. In this paper, a differential quadrature based numerical scheme is developed for solving volterra partial integro-differential equation of second order having a weakly singular kernel. The scheme uses cubic trigonometric B-spline functions to determine the weighting coefficients in the differential quadrature approximation of the second order spatial derivative. The advantage of this approximation is that it reduces the problem to a first order time dependent integro-differential equation (IDE). The proposed scheme is obtained in the form of an algebraic system by reducing the time dependent IDE through unconditionally stable Euler backward method as time integrator. The scheme is validated using a homogeneous and two nonhomogeneous test problems. Conditioning of the system matrix and numerical convergence of the method are analyzed for spatial and temporal domain discretization parameters. Comparison of results of the present approach with Sinc collocation method and quasi-wavelet method are also made.

Keywords: Partial integro-differential equation, differential quadrature, cubic trigonometric B-spline functions, weakly singular kernel.

1 Introduction

Partial integro-differential equations (PIDEs) are widely used to model several physical systems in science and engineering such as heat conduction [Gurtin and Pipkin (1968); Miller (1978)], reactor dynamics [Pao (1979)], flow in fractured biomaterials [Zadeh (2011)], electricity swaptions [Hepperger (2012)], population dynamics [Fakhar-Izadi and Dehghan (2013)], financial option pricing [Lee (2014)], viscoelasticity [Larsson, Racheva

¹ Department of Basic Sciences and Islamiat, University of Engineering and Technology Peshawar, Khyber Pakhtunkhwa, Pakistan.

² Department of Mathematics, Islamia College Peshawar, Khyber Pakhtunkhwa, Pakistan.

* Corresponding Author: Arshed Ali. Email: arshad.ali@icp.edu.pk.

Received: 27 April 2020; Accepted: 16 June 2020.

and Saedpanah (2015)] and diffusion [Ali, Rahman, Jan et al. (2016); Fahim, Araghi, Rashidinia et al. (2017)].

General solution in analytical form is usually possible under restrictive conditions. Such restrictive conditions often leading to over simplifications and compromising on the physical relevancy of the model. Thus, several alternative techniques have been appeared in the literature to obtain the solution of PIDEs, which include Galerkin methods [Fakhar-Izadi and Dehghan (2013); Larsson, Racheva and Saedpanah (2015)], radial basis function collocation method [Ali, Rahman, Jan et al. (2016)], Sinc-collocation method [Fahim, Araghi, Rashidinia et al. (2017)], finite element method [Chen, Thomee and Wahlbin (1992)], finite difference methods [Dehghan (2006); Tang (1993)], spectral method [Fakhar-Izadi and Dehghan (2011)], quasi-wavelet method [Long, Xu and Zeng (2012)], Haar wavelet method [Siraj-ul-Islam, Aziz and Fayyaz (2013)], and B-spline collocation methods [Zhang, Han and Yang (2013); Ahmad, Ali, Shah et al. (2015)].

The following second order PIDE is considered here [Fahim, Araghi, Rashidinia et al. (2017); Long, Xu and Zeng (2012)]:

$$\frac{\partial u(x, t)}{\partial t} = \int_0^t K(r, t) \frac{\partial^2 u(x, r)}{\partial x^2} dr + f(x, t), x \in I=[a, b], t > 0, \quad (1)$$

with initial condition

$$u(x, 0) = \psi(x), x \in I, \quad (2)$$

and boundary conditions

$$u(a, t) = \psi_1(t), u(b, t) = \psi_2(t), t > 0, \quad (3)$$

where $K(r, t) = (t-r)^{-\nu}$, $0 < \nu < 1$, is the weakly singular kernel. The term $\int_0^t K(r, t) \frac{\partial^2 u(x, r)}{\partial x^2} dr$ is called memory term which represents memory of the system in model. Different numerical techniques were proposed to obtain the solution of the PIDE (1). Fahim et al. [Fahim, Araghi, Rashidinia et al. (2017)] employed Sinc function to the spatial derivative and product trapezoidal rule to the time derivative to solve the PIDE (1). Dehghan [Dehghan (2006)] used finite difference schemes alongwith product trapezoidal numerical integration for its solution. Long et al. [Long, Xu and Zeng (2012)] obtained a technique based on quasi-wavelet for the solution of the PIDE (1). Shakeel et al. [Ahmad, Ali, Shah et al. (2015)] solved (1) through a quintic B-spline collocation method. Recently, Ali et al. [Ali, Khan, Haq et al. (2019)] constructed a collocation method based on cubic trigonometric B-spline functions to obtain the solution of the problem (1).

In 1964, Schoenberg [Schoenberg (1964)] presented piecewise trigonometric spline functions and established the existence of locally supported trigonometric splines, termed as trigonometric B-splines. Later on other researchers (see [Koch, Lyche, Neamtu et al.

(1995); Walz (1997)) developed further important properties of these functions such as C^2 continuity, nonnegativity, partition of unity, smoothness, curve shape design and its analysis, and recurrence relation. In 2010, Abd Hamid et al. [Abd Hamid, Majid and Ismail (2010)] pioneered the application of cubic trigonometric B-spline (CTBS) functions for the solution of Two-point boundary value problem. Due to their special features and better accuracy, CTBS based methods are extended for the solution of several partial differential equations including hyperbolic problems [Abbas, Majid, Ismail et al. (2014a)], Nonclassical diffusion problems [Abbas, Majid, Ismail et al. (2014b)], Burgers' equations [Raslan, El-Danaf and Ali (2016)], Hyperbolic telegraph equation [Nazir, Abbas and Yaseen (2017)], Hunter Saxton equation [Hashmi, Awais, Waheed et al. (2017)], Fisher's equations [Hepson and Dag (2017); Tamsir, Dhiman and Srivastava (2018)], time fractional diffusion-wave equation [Yaseen, Abbas, Nazir et al. (2017)], Non-conservative linear transport problem [Korkmaz and Akmaz (2018)], and coupled Burgers' equations [Dag, Hepson and Kacmaz (2017); Singh and Kumar (2018)].

In 1971, Bellman et al. [Bellman and Casti (1971)] introduced the DQ method for approximation of derivative of a sufficiently smooth function. This method is considered as strong alternative of finite difference and finite element methods since it produces accurate numerical results with little computational effort as compared to these methods because it uses relatively smaller set of nodal points [Quan and Chang (1989); Bert and Malik (1996)]. Various theoretical results and applications of this method can be found in the references [Shu (2000); Wang (2015)]. The method is utilized for the solution of various problems including Fisher's reaction-diffusion equations [Tamsir, Dhiman and Srivastava (2018)], Non-conservative linear transport problems [Korkmaz and Akmaz (2018)], coupled viscous Burger's equations [Singh and Kumar (2018)], Kawahara equation [Bashan (2019a)], Semi-linear Fisher-Kolmogorov equations [Mittal and Dahiya (2016)], cmKdV equation [Başhan, Yağmurlu, Uçar et al. (2018)], Boundary layer problems [Shen (2010)], shock wave simulations [Korkmaz and Dag (2011b)], and Burgers' equation [Arora and Singh (2013)].

Recently, Korkmaz et al. [Korkmaz and Akmaz (2018)] introduced the CTBS-DQ method for the solution of non-conservative linear transport problems based on second order advection-diffusion equation. Singh et al. [Singh and Kumar (2018)] extended the method for the solution of one and two dimensional coupled viscous Burgers' equations. Tasmir et al. [Tamsir, Dhiman and Srivastava (2018)] used the CTBS-DQ method for second order nonlinear Fisher's reaction-diffusion equations.

The aim of this work is to initiate the CTBS-DQ approach for the solution of PDIEs (1)-(3). Besides other challenges in solving PDEs, PIDEs of the form (1) have additional two major issues, the singular kernel and the memory term. These issues also require numerical treatment, which further affect stability and accuracy of a numerical method.

Rest of the paper is outlined as follows: Section 2 describes development of the proposed technique by coupling CTBS functions with differential quadrature method. Section 3 implements the CTBS-DQ method using test problems. This section also provides detail

error analysis, conditioning, eigenvalues, comparison with some existing methods, and computational efficiency in order to establish the current approach. Section 4 concludes the findings and outcomes of the paper.

2 The CTBS-DQ method

To develop the proposed method, consider the problem (1)-(3). We divide the spatial domain I into $N-1$ subintervals $I_n=[x_{n-1}, x_n]$, $n=2, 3, \dots, N$, of equal length $h=\frac{b-a}{N-1}$ by the collocation points x_n , $n \in \Omega=\{1, 2, \dots, N\}$ with $a=x_1$ and $b=x_N$. Taking $x=x_i$, $i \in \Omega$, in Eq. (1),

$$\frac{\partial u(x_i, t)}{\partial t} = \int_0^t K(r, t) \frac{\partial^2 u(x_i, r)}{\partial x^2} dr + f(x_i, t). \quad (4)$$

Next we use the differential quadrature to approximate $\frac{\partial^2 u(x_i, r)}{\partial x^2}$ using CTBS functions as follows.

The DQ method approximates k th order derivative of the function $u(x, r)$ from its values at x_i , $i \in \Omega$, as

$$\frac{\partial^k u(x_i, r)}{\partial x^k} = \sum_{j=1}^N a_{ij}^{(k)} u(x_j, r), \quad (5)$$

where $a_{ij}^{(k)}$, $k=1, 2, \dots$, are k th order weighting coefficients which are determined by test functions. Different basis functions were considered as test functions for determination of the weighting coefficients such as cubic trigonometric B-spline functions [Korkmaz and Akmaz (2018); Singh and Kumar (2018)], Lagrange polynomials [Quan and Chang (1989)], quintic B-spline functions [Mittal and Dahiya (2016)], sinc functions [Korkmaz and Dag (2011b)], cubic B-spline functions [Arora and Singh (2013); Bashan (2019b)], radial basis functions [Lin, Zhao, Watson et al. (2020); Shu, Ding and Yeo (2003)], Fourier expansion [Shu and Chew (1997)], and polynomial basis [Korkmaz and Dag (2011a)]. Accuracy of DQ solution depends on the accuracy of weighting coefficients and as well as on the selection of nodal points x_i . Moreover, the DQ solution declines with increasing the number of nodes which is a limitation of this method. Various researchers have provided different techniques such as using explicit formulae for computation of weighting coefficients of higher order derivatives and non-uniform nodes to circumvent this problem, which leads to improvement in accuracy of the DQ solution [Bert and Malik (1996)]. Shu [Shu (2000)] established two approaches (i) a recurrence formula (ii) matrix multiplication, for finding the weighting coefficients of derivatives of higher order. Recently, Lin et al. [Lin, Zhao, Watson et al. (2020)] presented an improved radial basis functions based DQ method using ghost points for the solution of 2D and 3D elliptic boundary value problems.

CTBS function denoted by $B_i(x)$ are given by Abd Hamid et al. [Abd Hamid, Majid and Ismail (2010)] and Abbas et al. [Abbas, Majid, Ismail et al. (2014a)]:

$$B_i(x) = \frac{1}{\omega} \begin{cases} \phi_{i-2}^3, & x \in I_{i-1}, \\ \phi_{i-2}[\phi_{i-2}\sigma_i + \sigma_{i+1}\phi_{i-1}] + \sigma_{i+1}\phi_{i-1}^2, & x \in I_i, \\ \phi_{i-2}\sigma_{i+1}^2 + \sigma_{i+2}(x)[\phi_{i-1}\sigma_{i+1} + \sigma_{i+2}\phi_i], & x \in I_{i+1}, \\ \sigma_{i+2}^3, & x \in I_{i+2}, \\ 0, & \text{otherwise,} \end{cases}$$

where $\phi_i = \sin\left(\frac{x-x_i}{2}\right)$, $\sigma_i = \sin\left(\frac{x_i-x}{2}\right)$, and $w = \sin\left(\frac{h}{2}\right) \sin(h) \sin\left(\frac{3h}{2}\right)$.

Lemma [Abd Hamid, Majid and Ismail (2010); Abbas, Majid, Ismail et al. (2014a)]: The value of $B_i(x)$, $B'_i(x)$ and $B''_i(x)$ at the node x_j are obtained as:

$$B_i(x_j) = \begin{cases} \beta_2, & \text{if } i-j=0, \\ \beta_1, & \text{if } i-j=1 \text{ or } -1, \\ 0, & \text{elsewhere,} \end{cases}$$

$$B'_i(x_j) = \begin{cases} \beta_4, & \text{if } i-j=1, \\ \beta_3, & \text{if } i-j=-1, \\ 0, & \text{elsewhere,} \end{cases}$$

and

$$B''_i(x_j) = \begin{cases} \beta_6, & \text{if } i-j=0, \\ \beta_5, & \text{if } i-j=1 \text{ or } -1, \\ 0, & \text{elsewhere,} \end{cases}$$

where

$$\beta_1 = \frac{\sin^2\left(\frac{h}{2}\right)}{\sin(h) \sin\left(\frac{3h}{2}\right)}, \beta_2 = \frac{2}{1+2\cos(h)}, \beta_3 = -\frac{3}{4\sin\left(\frac{3h}{2}\right)}, \beta_4 = \frac{3}{4\sin\left(\frac{3h}{2}\right)}$$

$$\beta_5 = \frac{3(1+3\cos(h))}{16(2\cos\left(\frac{h}{2}\right) + \cos\left(\frac{3h}{2}\right)) \sin^2\left(\frac{h}{2}\right)}, \text{ and } \beta_6 = -\frac{3\cot^2\left(\frac{h}{2}\right)}{2+4\cos(h)}$$

The following modified CTBS functions are used as test functions [Arora and Joshi (2018)]:

$$T_1(x) = (B_1 + 2B_0)(x),$$

$$T_2(x) = (B_2 - B_0)(x),$$

$$T_l(x) = B_l(x), \text{ for } l=3, 4, \dots, N-2,$$

$$T_{N-1}(x) = (B_{N-1} - B_{N+1})(x),$$

$$T_N(x) = (B_N + 2B_{N+1})(x),$$

which form a basis in region $[a, b]$.

Thus, for each basis function $T_m(x_i)$, Eq. (5) gives

$$\frac{\partial^k T_m(x_i)}{\partial x^k} = \sum_{j=1}^N a_{ij}^{(k)} T_m(x_j), \text{ for } m, i \in \Omega, \text{ and } k=2,$$

leading to the following matrix form:

$$C \vec{a}_i^{(k)} = D_i^{(k)}, \quad (6)$$

where $\vec{a}_i^{(k)} = [a_{ij}^{(k)}]_{j=1}^N$ and $D_i^{(k)} = \left[\frac{\partial^k T_m(x_i)}{\partial x^k} \right]_{m=1}^N$ are $N \times 1$ matrices while $C = [c_{ij}]_{i,j=1}^N$ is an $N \times N$ matrix such that

$$c_{ij} = \begin{cases} 2\beta_1 + \beta_2, & \text{if } i=j=1 \text{ or } N, \\ \beta_2, & \text{if } i=j \text{ and } 1 < i, j < N, \\ \beta_1, & \text{if } (j=i-1 \text{ and } 2 < i \leq N) \text{ or } (i=j-1 \text{ and } 1 \leq j < N-1), \\ 0, & \text{elsewhere.} \end{cases}$$

The weighting coefficients $a_{ij}^{(k)}$, $i, j \in \Omega$ are obtained by solving the system (6) through the well known efficient tridiagonal solver ‘‘Thomas algorithm’’. Thus using Eq. (5) in Eq. (4) and taking $K(r,t) = (t-r)^{-\nu}$, $k=2$, we get the following IDE,

$$\frac{\partial u(x_i, t)}{\partial t} = \int_0^t (t-r)^{-\nu} \sum_{j=1}^N a_{ij}^{(2)} u(x_j, r) dr + f(x_i, t), \quad i \in \Omega. \quad (7)$$

Let $t^l = l\Delta t$, $l=0, 1, 2, \dots, L$, where Δt is time step. Taking $t = t^{l+1}$ in Eq. (7), and approximating the time derivative in Eq. (7) by Euler backward formula, we get

$$\frac{u(x_i, t^{l+1}) - u(x_i, t^l)}{\Delta t} = \int_0^{t^{l+1}} (t^{l+1} - r)^{-\nu} \sum_{j=1}^N a_{ij}^{(2)} u(x_j, r) dr + f(x_i, t^{l+1}), \quad i \in \Omega. \quad (8)$$

The numerical treatment of the memory term in Eq. (8) containing the weakly singular kernel is performed as [Ali, Khan, Haq et al. (2019)]:

$$\begin{aligned} & \int_0^{t^{l+1}} (t^{l+1} - r)^{-\nu} \sum_{j=1}^N a_{ij}^{(2)} u(x_j, r) dr = \int_0^{t^{l+1}} r^{-\nu} \sum_{j=1}^N a_{ij}^{(2)} u(x_j, t^{l+1} - r) dr, \\ & = \sum_{k=0}^l \int_{t^k}^{t^{k+1}} r^{-\nu} \sum_{j=1}^N a_{ij}^{(2)} u(x_j, t^{l+1} - r) dr, \\ & \approx \sum_{k=0}^l \sum_{j=1}^N a_{ij}^{(2)} u(x_j, t^{l-k+1}) \int_{t^k}^{t^{k+1}} r^{-\nu} dr, \end{aligned}$$

$$\approx \frac{(\Delta t)^{1-\nu}}{1-\nu} \sum_{k=0}^l \sum_{j=1}^N a_{ij}^{(2)} u(x_j, t^{l-k+1}) ((k+1)^{1-\nu} - k^{1-\nu}), \tag{9}$$

Putting Eq. (9) in Eq. (8), and denoting $u(x_i, t^{l+1})$ by u_i^{l+1} , we get

$$\frac{u_i^{l+1} - u_i^l}{\Delta t} = \sum_{k=0}^l b_k \sum_{j=1}^N a_{ij}^{(2)} u_j^{l-k+1} + f_i^{l+1}, \tag{10}$$

where $b_k = \frac{(\Delta t)^{1-\nu}}{1-\nu} ((k+1)^{1-\nu} - k^{1-\nu})$ such that $b_k \rightarrow 0$ as $k \rightarrow \infty$ and $f_i^{l+1} = f(x_i, t^{l+1})$, $i \in \Omega$.

Re-arranging the terms in Eq. (10), we have

$$u_i^{l+1} - b_0 \Delta t \sum_{j=1}^N a_{ij}^{(2)} u_j^{l+1} = u_i^l + \Delta t \left(\sum_{k=1}^l b_k \sum_{j=1}^N a_{ij}^{(2)} u_j^{l-k+1} + f_i^{l+1} \right), \quad i \in \Omega. \tag{11}$$

Eq. (11) leads to the following matrix form:

$$\mathbf{P}\mathbf{u}^{l+1} = \mathbf{Q}\mathbf{u}^l + \mathbf{F}, \quad l \geq 2, \tag{12}$$

where

$$\mathbf{P} = \begin{bmatrix} 1 - b_0 \Delta t a_{11}^{(2)} & -b_0 \Delta t a_{12}^{(2)} & -b_0 \Delta t a_{13}^{(2)} & \dots & -b_0 \Delta t a_{1N}^{(2)} \\ -b_0 \Delta t a_{21}^{(2)} & 1 - b_0 \Delta t a_{22}^{(2)} & -b_0 \Delta t a_{23}^{(2)} & \dots & -b_0 \Delta t a_{2N}^{(2)} \\ \vdots & \vdots & \vdots & \dots & \vdots \\ \vdots & \vdots & \vdots & \dots & \vdots \\ -b_0 \Delta t a_{N1}^{(2)} & -b_0 \Delta t a_{N2}^{(2)} & -b_0 \Delta t a_{N3}^{(2)} & \dots & 1 - b_0 \Delta t a_{NN}^{(2)} \end{bmatrix},$$

$$\mathbf{Q} = \begin{bmatrix} 1 + b_1 \Delta t a_{11}^{(2)} & b_1 \Delta t a_{12}^{(2)} & b_1 \Delta t a_{13}^{(2)} & \dots & b_1 \Delta t a_{1N}^{(2)} \\ b_1 \Delta t a_{21}^{(2)} & 1 + b_1 \Delta t a_{22}^{(2)} & b_1 \Delta t a_{23}^{(2)} & \dots & b_1 \Delta t a_{2N}^{(2)} \\ \vdots & \vdots & \vdots & \dots & \vdots \\ \vdots & \vdots & \vdots & \dots & \vdots \\ b_1 \Delta t a_{N1}^{(2)} & b_1 \Delta t a_{N2}^{(2)} & b_1 \Delta t a_{N3}^{(2)} & \dots & 1 + b_1 \Delta t a_{NN}^{(2)} \end{bmatrix},$$

$\mathbf{u}^l = [u_1^l, u_2^l, \dots, u_N^l]^T$, and $\mathbf{F} = [s_1, s_2, \dots, s_N]^T$, $s_i = \Delta t \left(\sum_{k=2}^l b_k \sum_{j=1}^N a_{ij}^{(2)} u_j^{l-k+1} + f_i^{l+1} \right)$, $i \in \Omega$.

Eq. (12) can be rewritten as

$$\mathbf{u}^{l+1} = \mathbf{M}\mathbf{u}^l + \mathbf{G}, \tag{13}$$

where $\mathbf{M} = \mathbf{P}^{-1}\mathbf{Q}$ and $\mathbf{G} = \mathbf{P}^{-1}\mathbf{F}$.

3 Test problems

In this section three examples are taken from the literature [Fahim, Araghi, Rashidinia et al. (2017); Long, Xu and Zeng (2012)] with $\nu = \frac{1}{2}$ and the spatial domain $I = [0, 1]$ to validate and compare results of the present technique (13) with the results of Sinc-collocation method-Linsolve Package (SMLP) [Fahim, Araghi, Rashidinia et al. (2017)], Sinc-collocation method-Tikhonov Regularization (SMTR) [Fahim, Araghi, Rashidinia et al. (2017)] and quasi-wavelet (QW) method [Long, Xu and Zeng (2012)]. The method is examined via E_∞ , E_2 error norms [Ali, Khan, Haq et al. (2019)].

3.1 Problem 1

We take Eqs. (1)-(3) and choose $f(x,t)=0$ with the analytical solution [Fahim, Araghi, Rashidinia et al. (2017)]:

$$u(x, t) = \sum_{k=0}^{\infty} (-1)^k \nu \left(\frac{3}{2}k + 1 \right)^{-1} (\pi^{5/2} t^{3/2})^k \sin(\pi x). \quad (14)$$

The functions ψ , ψ_1 , ψ_2 are obtained from Eq. (14). Simulation is done with different values of the parameter N , time step Δt , time level L , and the results of CTBS-DQ are provided in Tabs. 1-5 along with the results of the methods SMLP, SMTR [Fahim, Araghi, Rashidinia et al. (2017)]. From Tabs. 1 and 2, it can be seen that CTBS-DQ method produces better accuracy than SMLP [Fahim, Araghi, Rashidinia et al. (2017)] for $\Delta t = 10^{-4}$, whereas it gives comparable accuracy to SMTR [Fahim, Araghi, Rashidinia et al. (2017)]. Furthermore, it can be noted from Tab. 1 that condition number of the system matrix \mathbf{P} ($\text{Cond}(\mathbf{P})$) in Eq. (12) is much smaller than the sinc-collocation method [Fahim, Araghi, Rashidinia et al. (2017)] for all values of $N=9, 17, 33, 65, 100, 500$. In Tab. 3, the error norms are obtained for $L=50, 150, 250, 350, 450, 1000$ using $\Delta t = 10^{-4}, 10^{-5}$. In Tab. 4, Spatial rate of convergence, condition number of weighting coefficient matrix \mathbf{A} , $\rho(\mathbf{A})$ and $\rho(\mathbf{M})$ spectral radii of matrices \mathbf{A} and \mathbf{M} respectively, are recorded for $N=10, 20, 50, 100, 500$. Both $\text{Cond}(\mathbf{A})$ and $\rho(\mathbf{A})$ increase as N increases but $\rho(\mathbf{M})$ of the amplification matrix \mathbf{M} remains 1, which shows stable computation. In Tab. 5, time rate of convergence, condition numbers of the system matrix \mathbf{P} and amplification matrix \mathbf{M} and $\rho(\mathbf{M})$ spectral radius of matrix \mathbf{M} are given for $\Delta t = 10^{-2}, 10^{-3}, 10^{-4}, 10^{-5}, 10^{-6}$. It can be observed from the Tab. 5 that both $\text{Cond}(\mathbf{P})$ and $\text{Cond}(\mathbf{M})$ approach to 1 as Δt decreases, while $\rho(\mathbf{M})$ remains 1. Fig. 1 represents solution obtained by CTBS-DQ at $t=0.1$. Fig. 2 displays errors in approximation obtained by the present methods. Fig. 3 shows the CTBS-DQ solutions at different time levels upto $t=0.1$. Fig. 4 represents convergence of CTBS-DQ solution and condition number of the matrix \mathbf{M} vs. spatial nodes N .

Table 1: Results of CTBS-DQ using $\Delta t=10^{-4}$ at $t=0.01$ alongwith results of the methods [Fahim, Araghi, Rashidinia et al. (2017)]

N	CTBS-DQ			[Fahim, Araghi, Rashidinia et al. (2017)]		
	E_∞	E_2	Cond(P)	E_∞ (SMLP)	E_∞ (SMTR)	Cond(P)
9	2.20×10^{-4}	1.56×10^{-4}	1.00×10^0	1.10×10^{-2}	8.27×10^{-3}	4.61×10^2
17	1.24×10^{-4}	8.79×10^{-5}	1.01×10^0	2.85×10^{-3}	7.94×10^{-4}	6.71×10^3
33	1.00×10^{-4}	7.10×10^{-5}	1.02×10^0	4.68×10^{-4}	9.32×10^{-5}	3.88×10^4
65	9.44×10^{-5}	6.68×10^{-5}	1.10×10^0	9.75×10^{-5}	4.71×10^{-5}	1.10×10^5
100	9.32×10^{-5}	6.60×10^{-5}	1.35×10^0
500	9.25×10^{-5}	6.54×10^{-5}	2.77×10^3

Table 2: Pointwise absolute error at $t=1$ using $N=10$

x	$\Delta t=10^{-2}$		$\Delta t=10^{-3}$		$\Delta t=10^{-4}$	
	CTBS-DQ	SMLP	CTBS-DQ	SMLP	CTBS-DQ	SMLP
0.1	3.3×10^{-3}	1.9×10^{-3}	3.6×10^{-4}	4.1×10^{-4}	4.2×10^{-5}	2.6×10^{-4}
0.2	6.3×10^{-3}	3.4×10^{-3}	6.8×10^{-4}	6.1×10^{-4}	8.0×10^{-5}	3.1×10^{-4}
0.3	8.7×10^{-3}	4.4×10^{-3}	9.4×10^{-4}	5.3×10^{-4}	1.1×10^{-4}	1.3×10^{-4}
0.4	1.0×10^{-2}	5.1×10^{-3}	1.1×10^{-3}	4.9×10^{-4}	1.3×10^{-4}	1.1×10^{-4}
0.5	1.1×10^{-2}	5.3×10^{-3}	1.2×10^{-3}	4.9×10^{-4}	1.4×10^{-4}	1.7×10^{-4}
0.6	1.0×10^{-2}	5.1×10^{-3}	1.1×10^{-3}	4.9×10^{-4}	1.3×10^{-4}	1.1×10^{-4}
0.7	8.7×10^{-3}	4.4×10^{-3}	9.4×10^{-4}	5.3×10^{-4}	1.1×10^{-4}	1.3×10^{-4}
0.8	6.3×10^{-3}	3.4×10^{-3}	6.8×10^{-4}	6.1×10^{-4}	8.0×10^{-5}	3.1×10^{-4}
0.9	3.3×10^{-3}	1.9×10^{-3}	3.6×10^{-4}	4.1×10^{-4}	4.2×10^{-5}	2.6×10^{-4}

Table 3: Error norms obtained by CTBS-DQ using $N=20$

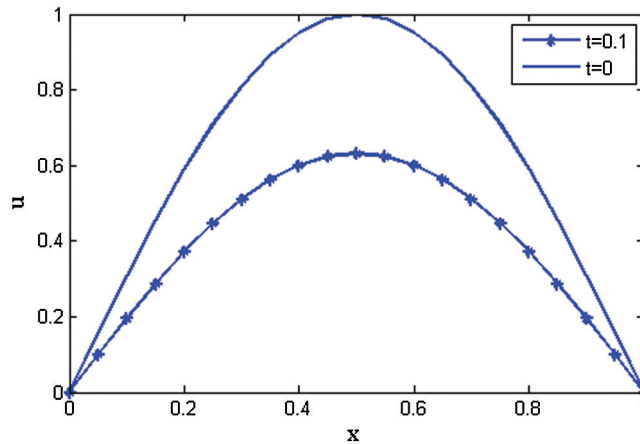
L	$\Delta t=10^{-4}$		$\Delta t=10^{-5}$		CPU Time (s)
	E_∞	E_2	E_∞	E_2	
50	7.25×10^{-5}	5.13×10^{-5}	2.31×10^{-6}	1.63×10^{-6}	0.0294
150	1.49×10^{-4}	1.05×10^{-4}	4.88×10^{-6}	3.45×10^{-6}	0.0327
250	2.16×10^{-4}	1.53×10^{-4}	7.34×10^{-6}	5.19×10^{-6}	0.0496
350	2.81×10^{-4}	1.99×10^{-4}	9.90×10^{-6}	7.00×10^{-6}	0.0644
450	3.42×10^{-4}	2.42×10^{-4}	1.26×10^{-5}	8.90×10^{-6}	0.0879
1000	6.15×10^{-4}	4.35×10^{-4}	2.98×10^{-5}	2.10×10^{-5}	0.3079

Table 4: Convergence of CTBS-DQ solution in space using $\Delta t=10^{-4}$ at $t=0.01$

N	E_∞	E_2	Order (E_∞)	Cond(A)	$\rho(A)$	$\rho(M)$
10	9.06×10^{-5}	6.04×10^{-5}	—	5.58×10^6	1.12×10^3	1.0000
20	2.97×10^{-5}	2.10×10^{-5}	1.6075	1.30×10^8	4.71×10^3	1.0000
50	1.27×10^{-5}	9.01×10^{-6}	0.9243	8.06×10^9	2.99×10^4	1.0000
100	1.03×10^{-5}	7.30×10^{-6}	0.3043	1.82×10^{11}	1.20×10^5	1.0000
500	9.54×10^{-6}	6.75×10^{-6}	0.0485	2.54×10^{14}	3.00×10^6	1.0000

Table 5: Convergence of CTBS-DQ solution in time using $N=20$ at $t=0.01$

Δt	E_∞	E_2	Order (E_∞)	Cond(P)	Cond(M)	$\rho(M)$
10^{-2}	6.28×10^{-3}	4.44×10^{-3}	— — —	1.16×10^1	6.53×10^2	1.0000
10^{-3}	8.65×10^{-4}	6.11×10^{-4}	0.8609	1.30×10^0	1.44×10^0	1.0000
10^{-4}	1.13×10^{-4}	7.98×10^{-5}	0.8845	1.01×10^0	1.01×10^0	1.0000
10^{-5}	2.97×10^{-5}	2.10×10^{-5}	0.5794	1.00×10^0	1.00×10^0	1.0000
10^{-6}	2.12×10^{-5}	1.50×10^{-5}	0.1470	1.00×10^0	1.00×10^0	1.0000

**Figure 1:** Numerical solutions obtained by CTBS-DQ using $N=20$, $\Delta t=10^{-4}$ at $t=0.1$

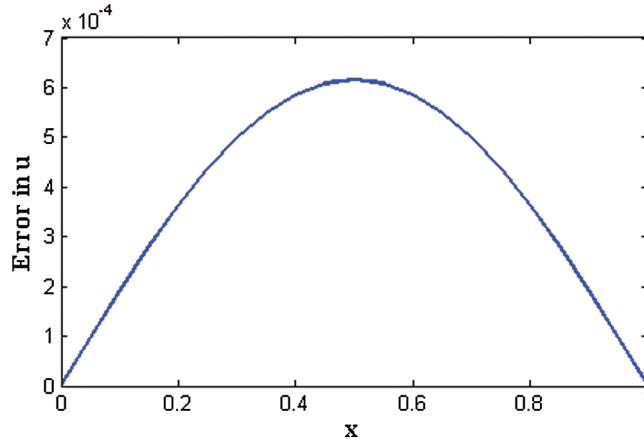


Figure 2: Error in numerical solutions obtained by CTBS-DQ using $N=20$, $\Delta t=10^{-4}$ at $t=0.1$

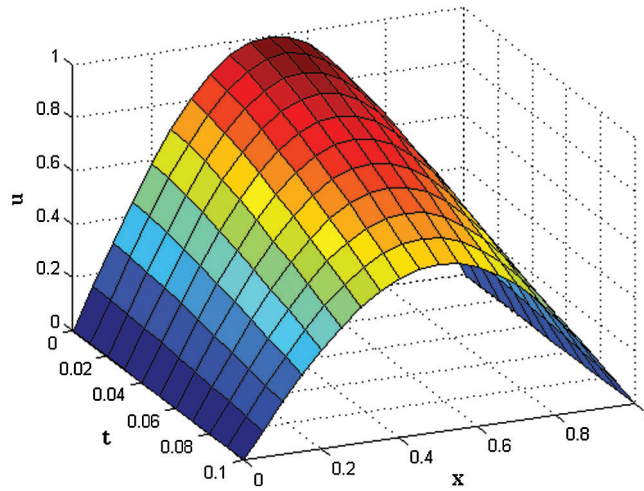


Figure 3: CBTS-DQ solutions at different time levels in $[0, 0.1]$ using $N=20$, $\Delta t=10^{-4}$ at $t=0.1$

3.2 Problem 2

We consider Eqs. (1)-(3) with

$$f(x, t) = \frac{2t^{1/2}}{\sqrt{\pi}} (\pi^2 \sin \pi x - \sin 2\pi x) - 2\pi^2 t^2 \sin 2\pi x,$$

$\psi(x)=\sin(\pi x)$, $\psi_1(t)=0$, $\psi_2(t)=0$, and in this case the exact solution is given by Fahim et al. [Fahim, Araghi, Rashidinia et al. (2017); Long, Xu and Zeng (2012)]

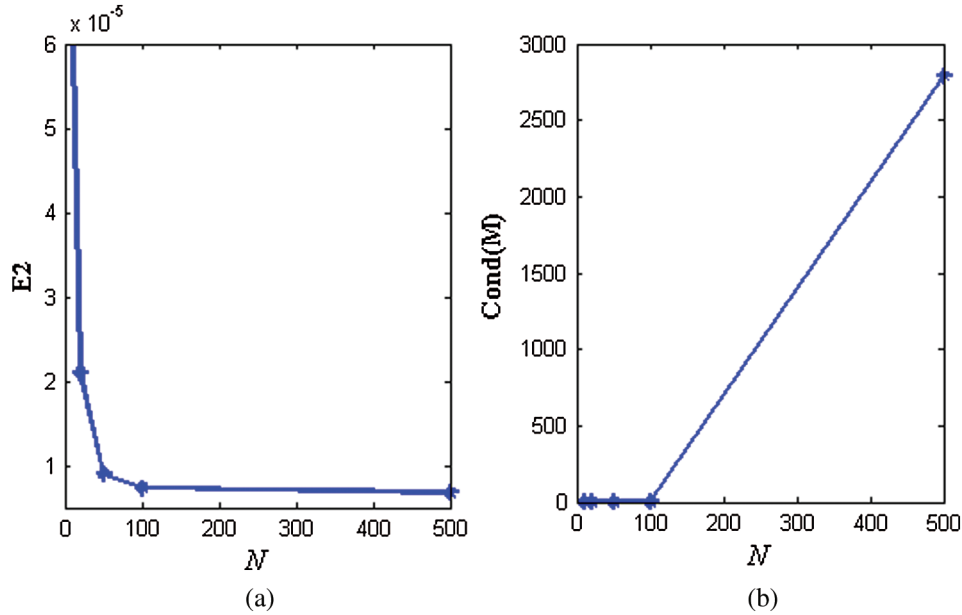


Figure 4: (a) Convergence of CTBS-DQ solution vs. number of spatial nodes N (b) Condition number of amplification matrix M vs. N , for $\Delta t=10^{-4}$ at $t=0.1$

$$u(x, t) = \sin(\pi x) - \frac{4t^{3/2}}{3\sqrt{\pi}} \sin 2\pi x. \tag{15}$$

The error norms for $N=10, 65, \Delta t=10^{-5}, 10^{-6}$ and at time level $L=50, 150, 250, 350, 450$ are computed through the CTBS-DQ (13) which are provided in Tab. 6 along with the results of QW [Long, Xu and Zeng (2012)] and SMLP [Fahim, Araghi, Rashidinia et al. (2017)]. From Tab. 6, it can be noted that the results produced by the CTBS-DQ are more accurate than QW [Long, Xu and Zeng (2012)] whereas CTBS-DQ gives comparable accuracy for less number of spatial nodes than SMLP [Fahim, Araghi, Rashidinia et al. (2017)]. Fig. 5 depicts solution obtained by the present method at $t=0.01$. Fig. 6 shows the CTBS-DQ solutions at various time levels up to $t=0.01$.

3.3 Problem 3

In this test problem we take Eqs. (1)-(3) with the singular kernel $K(r, t) = (\pi(t-r))^{-\frac{1}{2}}$, $f(x, t) = \sin(\pi x)$, $\psi(x) = \sin(\pi x)$, $\psi_1(t) = 0$, $\psi_2(t) = 0$ and the following analytical solution [Fahim, Araghi, Rashidinia et al. (2017)]

Table 6: Error norms at t=0.01

		CTBS-DQ		CTBS-DQ		QW	SMLP
		N=10		N=65		N=10	N=65
Δt	L	E_∞	E_2	E_∞	E_2	E_∞	E_∞
10^{-5}	50	6.60×10^{-5}	4.66×10^{-5}	6.50×10^{-5}	4.60×10^{-5}	4.93×10^{-4}	5.16×10^{-5}
	150	3.40×10^{-4}	2.40×10^{-4}	3.35×10^{-4}	2.37×10^{-4}	2.52×10^{-3}	2.90×10^{-4}
	250	7.29×10^{-4}	5.15×10^{-4}	7.19×10^{-4}	5.08×10^{-4}	5.36×10^{-3}	6.42×10^{-4}
	350	1.21×10^{-3}	8.53×10^{-4}	1.19×10^{-3}	8.41×10^{-4}	8.76×10^{-3}	1.08×10^{-3}
	450	1.76×10^{-3}	1.24×10^{-3}	1.73×10^{-3}	1.22×10^{-3}	1.26×10^{-2}	1.59×10^{-3}
10^{-6}	50	2.08×10^{-6}	1.47×10^{-6}	2.06×10^{-6}	1.45×10^{-6}	1.56×10^{-5}	9.81×10^{-6}
	150	1.07×10^{-5}	7.59×10^{-6}	1.06×10^{-5}	7.49×10^{-6}	8.05×10^{-5}	9.81×10^{-6}
	250	2.31×10^{-5}	1.63×10^{-5}	2.27×10^{-5}	1.61×10^{-5}	1.73×10^{-4}	2.03×10^{-5}
	350	3.82×10^{-5}	2.70×10^{-5}	3.76×10^{-5}	2.66×10^{-5}	2.86×10^{-4}	3.42×10^{-5}
	450	5.56×10^{-5}	3.93×10^{-5}	5.48×10^{-5}	3.88×10^{-5}	4.16×10^{-4}	5.03×10^{-5}

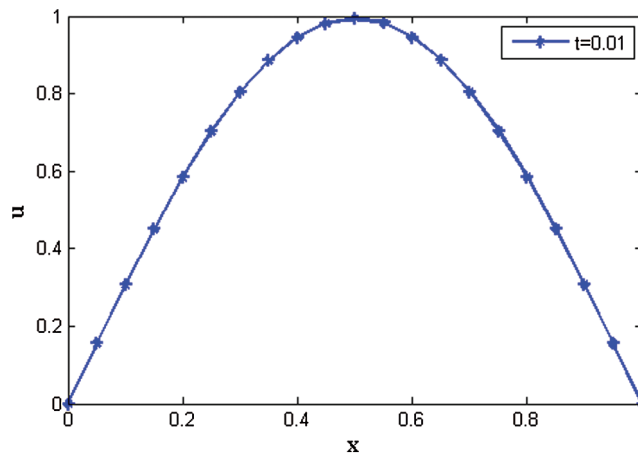


Figure 5: Numerical solution obtained by CTBS-DQ using $N=20$, $\Delta t=10^{-5}$, at $t=0.01$

$$u(x, t) = \left(\sum_{k=0}^{\infty} (-1)^k \frac{(\pi^2 t^{3/2})^k}{v\left(1 + \frac{3}{2}k\right)} + t \sum_{k=0}^{\infty} (-1)^k \frac{(\pi^2 t^{3/2})^k}{v\left(2 + \frac{3}{2}k\right)} \right) \sin \pi x.$$

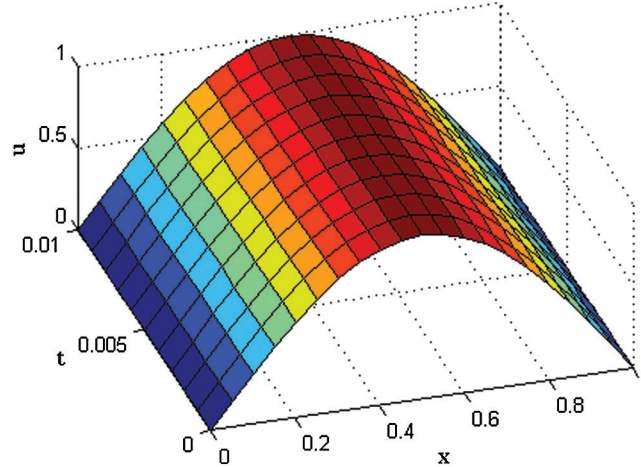


Figure 6: CTBS-DQ solutions at various times in $[0, 0.01]$ using $N=20$, $\Delta t=10^{-4}$

For this kernel the proposed scheme (12) and (13) is applied with the matrices

$$\mathbf{P} = \left[\mathbf{I} - \frac{2b_0(\Delta t)^{\frac{3}{2}}}{\sqrt{\pi}} \mathbf{A} \right], \quad \mathbf{Q} = \left[\mathbf{I} + \frac{2b_1(\Delta t)^{\frac{3}{2}}}{\sqrt{\pi}} \mathbf{A} \right], \quad \mathbf{A} = [a_{ij}^{(2)}]_{i,j=1}^N, \quad \mathbf{I} \text{ is } N \times N \text{ identity matrix and}$$

$$\mathbf{F} = \frac{\Delta t}{\sqrt{\pi}} [s_1, s_2, \dots, s_N]^T. \text{ The error norms for } N=17, 129, \Delta t=10^{-5}, 10^{-6}, 10^{-7} \text{ and } L=50,$$

150, 250, 350, 450 are obtained which are recorded in Tab. 7 along with results of SMLP [Fahim, Araghi, Rashidinia et al. (2017)] and SMTR [Fahim, Araghi, Rashidinia et al. (2017)]. From Tab. 7, accuracy of the CTBS-DQ increases as the time step Δt decreases but it does not increase by increasing of the number of spatial nodes N . Furthermore, CTBS-DQ provided more accurate solution for $N=17$ as compared to the accuracy of SMLP [Fahim, Araghi, Rashidinia et al. (2017)] and SMTR [Fahim, Araghi, Rashidinia et al. (2017)] for $N=17$. However, SMLP [Fahim, Araghi, Rashidinia et al. (2017)] and SMTR [Fahim, Araghi, Rashidinia et al. (2017)] require $N=129$ to attain this accuracy of CTBS-DQ for all $L=50, 150, 250, 350$. Fig. 7 illustrates solution obtained using CTBS-DQ at $t=0.001$. In Fig. 8, error in the solution obtained by the present method at $t=0.001$ is shown. Fig. 9 shows the CTBSF-DQ solutions at different time levels upto $t=0.001$

Table 7: Results for Problem 3

		N=17		N=129		N=17		N=129	
		CTBS-DQ		CTBS-DQ		SMTR	SMLP	SMTR	SMLP
Δt	L	E_∞	E_2	E_∞	E_2	E_∞	E_∞	E_∞	E_∞
10^{-5}	50	6.28×10^{-5}	4.44×10^{-5}	6.29×10^{-5}	4.45×10^{-5}	8.52×10^{-4}	2.75×10^{-3}	3.41×10^{-6}	5.28×10^{-5}
	150	3.30×10^{-4}	2.33×10^{-4}	3.31×10^{-4}	2.34×10^{-4}	8.94×10^{-4}	2.83×10^{-3}	1.92×10^{-5}	2.92×10^{-4}
	250	7.12×10^{-4}	5.04×10^{-4}	7.14×10^{-4}	5.05×10^{-4}	9.86×10^{-4}	2.87×10^{-3}	4.56×10^{-5}	6.45×10^{-4}
	350	1.18×10^{-3}	8.35×10^{-4}	1.18×10^{-3}	8.38×10^{-4}	9.71×10^{-3}	2.88×10^{-3}	5.37×10^{-5}	1.08×10^{-3}
	450	1.72×10^{-3}	1.22×10^{-3}	1.73×10^{-3}	1.22×10^{-3}
10^{-6}	50	1.98×10^{-6}	1.40×10^{-6}	1.99×10^{-6}	1.41×10^{-6}	8.28×10^{-4}	1.05×10^{-3}	9.86×10^{-7}	1.67×10^{-6}
	150	1.04×10^{-5}	7.38×10^{-6}	1.05×10^{-5}	7.40×10^{-6}	8.41×10^{-4}	2.58×10^{-3}	5.17×10^{-6}	9.24×10^{-6}
	250	2.25×10^{-5}	1.59×10^{-5}	2.23×10^{-5}	1.60×10^{-5}	9.73×10^{-4}	2.61×10^{-3}	6.84×10^{-6}	2.04×10^{-5}
	350	3.73×10^{-5}	2.64×10^{-5}	3.74×10^{-5}	2.65×10^{-5}	8.84×10^{-4}	2.61×10^{-3}	7.13×10^{-6}	3.43×10^{-5}
	450	5.45×10^{-5}	3.85×10^{-5}	5.46×10^{-5}	3.86×10^{-5}
10^{-7}	50	6.27×10^{-8}	4.44×10^{-8}	6.29×10^{-8}	4.45×10^{-8}	9.71×10^{-7}	3.57×10^{-6}	7.53×10^{-8}	6.11×10^{-8}
	150	3.30×10^{-7}	2.33×10^{-7}	3.31×10^{-7}	2.34×10^{-7}	7.34×10^{-6}	1.65×10^{-4}	8.91×10^{-8}	2.28×10^{-7}
	250	7.12×10^{-7}	5.03×10^{-7}	7.14×10^{-7}	5.05×10^{-7}	6.52×10^{-5}	4.35×10^{-4}	9.52×10^{-8}	6.45×10^{-7}
	350	1.18×10^{-6}	8.35×10^{-7}	1.18×10^{-6}	8.37×10^{-7}	1.41×10^{-4}	6.13×10^{-4}	1.54×10^{-7}	9.44×10^{-7}
	450	1.72×10^{-6}	1.22×10^{-6}	1.73×10^{-6}	1.22×10^{-6}

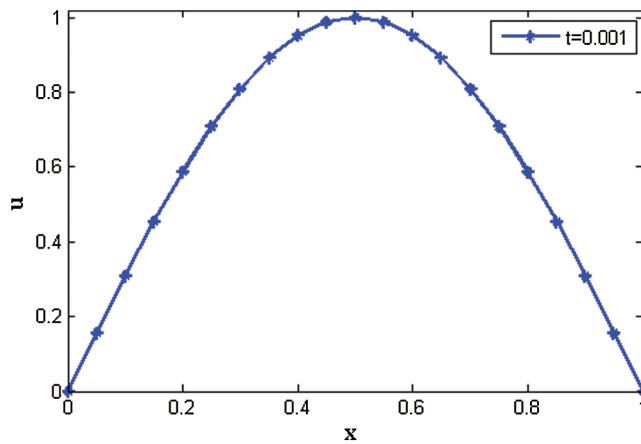


Figure 7: CTBS-DQ solution at $t=0.001$ using $N=20$, $\Delta t=10^{-5}$

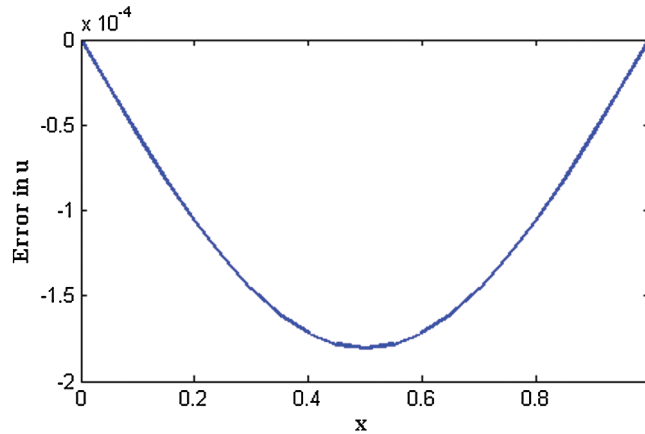


Figure 8: Error in CTBS-DQ solution at $t=0.001$ using $N=20$, $\Delta t=10^{-5}$

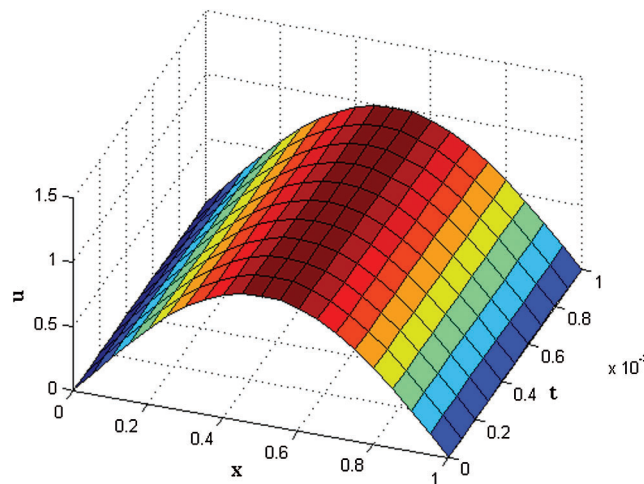


Figure 9: Numerical solutions obtained by CTBS-DQ at different times in $[0, 0.001]$ using $N=20$, $\Delta t=10^{-5}$

4 Conclusion

A differential quadrature based cubic trigonometric B-spline method is presented for approximate solution of a second order parabolic type partial integro-differential equation with a weakly singular kernel. Three test problems including two nonhomogeneous are provided for its validation, and the results are computed through error norms. The method is computationally efficient and improved accuracy is obtained for relatively small time step sizes. It is found that condition number of the system matrix does not increase with increase in the number of grid points and decreasing the time step size, and

thus leads to stable computation. The condition number of this method is sufficiently smaller than Sinc-collocation method. In most cases, it is observed that the present method provided better accuracy than Sinc-collocation methods when small number of spatial nodes and small time step are used. Also, the proposed method provided better accuracy than quasi-wavelet method. Due to excellent agreement of the method with the exact solution, the proposed technique is found efficient in obtaining approximate solution of this kind of PIDEs.

Acknowledgement: The authors are thankful to the reviewers for their helpful comments which improved the work of this paper.

Funding Statement: The authors received no specific funding for this study.

Conflicts of Interest: The authors declare that they have no conflicts of interest to report regarding the present study.

References

- Abbas, M.; Majid, A. A.; Ismail, A. I. M.; Rashid, A.** (2014a): The application of cubic trigonometric B-spline to the numerical solution of the hyperbolic problems. *Applied Mathematics and Computation*, vol. 239, pp. 74-88.
- Abbas, M.; Majid, A. A.; Ismail, A. I. M.; Rashid, A.** (2014b): Numerical method using cubic trigonometric B-spline technique for nonclassical diffusion problems. *Abstract and Applied Analysis*, vol. 2014, 849682.
- Abd Hamid, N. N.; Majid, A. A.; Ismail, A. I. M.** (2010): Cubic trigonometric B-spline applied to linear two-point boundary value problems of order two. *World Academy of Science, Engineering and Technology International Journal of Mathematical and Computational Sciences*, vol. 4, no. 10, pp. 1377-1382.
- Ahmad, S.; Ali, A.; Shah, S. I. A.; Haq, F.** (2015): A computational algorithm for the solution of second order partial integro-differential equations with a weakly singular kernel using quintic B-spline collocation method. *Sindh University Research Journal*, vol. 47, no. 4, pp. 709-712.
- Ali, A.; Khan, K.; Haq, F.; Shah, S. I. A.** (2019): A computational modeling based on trigonometric cubic B-spline functions for the approximate solution of a second order partial integro-differential. *New Knowledge in Information Systems and Technologies*. vol. 930, pp. 844-854. AISC, Spain: Springer Nature Switzerland.
- Ali, A.; Rahman, E.; Jan, Z.; Hussain, I.; Ahmad, S.** (2016): A meshless collocation method for the approximate solution of a partial integro-differential equation. *Sindh University Research Journal*, vol. 48, no. 3, pp. 589-594.
- Arora, G.; Joshi, V.** (2018): A computational approach using modified trigonometric cubic B-spline for numerical solution of Burgers' equation in one and two dimensions. *Alexandria Engineering Journal*, vol. 57, no. 2, pp. 1087-1098. DOI 10.1016/j.aej.2017.02.017.

- Arora, G.; Singh, B. K.** (2013): Numerical solution of Burgers' equation with modified cubic B-spline differential quadrature method. *Applied Mathematics and Computation*, vol. 224, pp. 166-177. DOI 10.1016/j.amc.2013.08.071.
- Bashan, A.** (2019a): An efficient approximation to numerical solutions for the Kawahara equation via modified cubic B-spline differential quadrature method. *Mediterranean Journal of Mathematics*, vol. 16, pp. 14.
- Bashan, A.** (2019b): A mixed algorithm for numerical computation of soliton solutions of the coupled KdV equation: finite difference method and differential quadrature method. *Applied Mathematics and Computation*, vol. 360, pp. 42-57.
- Başhan, A.; Yağmurlu, N. M.; Uçar, Y.; Esen, A.** (2018): A new perspective for the numerical solutions of the cmKdV equation via modified cubic B-spline differential quadrature method. *International Journal of Modern Physics C*, vol. 29, no. 6, pp. 1850043. DOI 10.1142/S0129183118500432.
- Bellman, R.; Casti, J.** (1971): Differential quadrature and long-term integration. *Journal of Mathematical Analysis and Applications*, vol. 34, no. 2, pp. 235-238. DOI 10.1016/0022-247X(71)90110-7.
- Bert, C. W.; Malik, M.** (1996): Differential quadrature method in computational mechanics: a review. *Applied Mechanics Reviews*, vol. 49, no. 1, pp. 1-28. DOI 10.1115/1.3101882.
- Chen, C.; Thomee, V.; Wahlbin, L. B.** (1992): Finite element approximation of a parabolic integro-differential equation with a weakly singular kernel. *Mathematics of Computation*, vol. 58, no. 198, pp. 587-602. DOI 10.1090/S0025-5718-1992-1122059-2.
- Dag, I.; Hepson, O. E.; Kacmaz, O.** (2017): The trigonometric cubic B-spline algorithm for Burgers' equation. *International Journal of Nonlinear Science*, vol. 24, no. 2, pp. 120-128.
- Dehghan, M.** (2006): Solution of a partial integro-differential equation arising from viscoelasticity. *International Journal of Computer Mathematics*, vol. 83, no. 1, pp. 123-129. DOI 10.1080/00207160500069847.
- Fahim, A.; Araghi, M. A. F.; Rashidinia, J.; Jalalvand, M.** (2017): Numerical solution of Volterra partial integro-differential equations based on sinc-collocation method. *Advances in Difference Equations*, vol. 2017, no. 1, pp. 481. DOI 10.1186/s13662-017-1416-7.
- Fakhar-Izadi, F.; Dehghan, M.** (2011): The spectral methods for parabolic Volterra integro-differential equations. *Journal of Computational and Applied Mathematics*, vol. 235, no. 14, pp. 4032-4046. DOI 10.1016/j.cam.2011.02.030.
- Fakhar-Izadi, F.; Dehghan, M.** (2013): An efficient pseudo-spectral Legendre-Galerkin method for solving a nonlinear partial integro-differential equation arising in population dynamics. *Mathematical Methods in the Applied Sciences*, vol. 36, no. 12, pp. 1485-1511. DOI 10.1002/mma.2698.

Gurtin, M. E.; Pipkin, A. C. (1968): A general theory of heat conduction with finite wave speeds. *Archive for Rational Mechanics and Analysis*, vol. 31, no. 2, pp. 113-126. DOI 10.1007/BF00281373.

Hashmi, M. S.; Awais, M.; Waheed, A.; Ali, Q. (2017): Numerical treatment of Hunter Saxton equation using cubic trigonometric B-spline collocation method. *AIP Advances*, vol. 7, no. 9, pp. 095124. DOI 10.1063/1.4996740.

Hepperger, P. (2012): Hedging electricity swaptions using partial integro-differential equations. *Stochastic Processes and their Applications*, vol. 122, no. 2, pp. 600-622. DOI 10.1016/j.spa.2011.09.005.

Hepson, O. E.; Dag, I. (2017): The numerical approach to the Fisher's equation via trigonometric cubic B-spline collocation method. *Communications in Numerical Analysis*, vol. 2017, no. 2, pp. 91-100. DOI 10.5899/2017/cna-00293.

Siraj-ul-Islam; Aziz, I.; Fayyaz, M. (2013): A new approach for numerical solution of integro-differential equations via Haar wavelets. *International Journal of Computer Mathematics*, vol. 90, no. 9, pp. 1971-1989. DOI 10.1080/00207160.2013.770481.

Koch, P.; Lyche, T.; Neamtu, M.; Schumaker, L. (1995): Control curves and knot insertion for trigonometric splines. *Advances in Computational Mathematics*, vol. 3, no. 4, pp. 405-424. DOI 10.1007/BF03028369.

Korkmaz, A.; Akmaz, H. K. (2018): Numerical solution of non-conservative linear transport problems. *Journal of Applied and Engineering Mathematics*, vol. 8, no. 1a, pp. 167-177.

Korkmaz, A.; Dag, I. (2011a): Polynomial based differential quadrature method for numerical solution of nonlinear Burgers' equation. *Journal of Franklin Institute*, vol. 348, no. 10, pp. 2863-2875.

Korkmaz, A.; Dag, I. (2011b): Shock wave simulations using Sinc differential quadrature method. *Engineering Computations*, vol. 28, no. 6, pp. 654-674.

Larsson, S.; Racheva, M.; Saedpanah, F. (2015): Discontinuous Galerkin method for an integro-differential equation modeling dynamic fractional order viscoelasticity. *Computer Methods in Applied Mechanics and Engineering*, vol. 283, pp. 196-209. DOI 10.1016/j.cma.2014.09.018.

Lee, Y. Y. (2014): Financial options pricing with regime-switching jump-diffusions. *Computers and Mathematics with Applications*, vol. 68, no. 3, pp. 392-404. DOI 10.1016/j.camwa.2014.06.015.

Lin, J.; Zhao, Y.; Watson, D.; Chen, C. S. (2020): The radial basis function differential quadrature method with ghost points. *Mathematics and Computers in Simulation*, vol. 173, pp. 105-114. DOI 10.1016/j.matcom.2020.01.006.

Long, W.; Xu, D.; Zeng, X. (2012): Quasi wavelet based numerical method for a class of partial integro-differential equation. *Applied Mathematics and Computation*, vol. 218, no. 24, pp. 11842-11850. DOI 10.1016/j.amc.2012.04.090.

- Miller, R. K.** (1978): An integrodifferential equation for rigid heat conductors with memory. *Journal of Mathematical Analysis and Applications*, vol. 66, no. 2, pp. 313-332. DOI 10.1016/0022-247X(78)90234-2.
- Mittal, R. C.; Dahiya, S.** (2016): A study of quintic B-spline based differential quadrature method for a class of semi-linear Fisher-Kolmogorov equations. *Alexandria Engineering Journal*, vol. 55, no. 3, pp. 2893-2899. DOI 10.1016/j.aej.2016.06.019.
- Nazir, T.; Abbas, M.; Yaseen, M.** (2017): Numerical solution of second-order hyperbolic telegraph equation via new cubic trigonometric B-splines approach. *Cogent Mathematics*, vol. 4, no. 1, pp. 1382061. DOI 10.1080/23311835.2017.1382061.
- Pao, C. V.** (1979): Bifurcation analysis of a nonlinear diffusion system in reactor dynamics. *Applicable Analysis*, vol. 9, no. 2, pp. 107-119. DOI 10.1080/00036817908839258.
- Quan, J. R.; Chang, C. T.** (1989): New insights in solving distributed system equations by the quadrature method I: analysis. *Computers and Chemical Engineering*, vol. 13, no. 7, pp. 779-788. DOI 10.1016/0098-1354(89)85051-3.
- Raslan, K. R.; El-Danaf, T. S.; Ali, K. K.** (2016): Collocation method with cubic trigonometric B-spline algorithm for solving coupled Burgers' equations. *Far East Journal of Applied Mathematics*, vol. 95, no. 2, pp. 109-123. DOI 10.17654/AM095020109.
- Schoenberg, I. J.** (1964): On trigonometric spline interpolation. *Journal of Mathematics and Mechanics*, vol. 13, pp. 795-825.
- Shen, Q.** (2010): Local RBF-based differential quadrature collocation method for the boundary layer problems. *Engineering Analysis with Boundary Elements*, vol. 34, no. 3, pp. 213-228. DOI 10.1016/j.enganabound.2009.10.004.
- Shu, C.** (2000): *Differential Quadrature and Its Application in Engineering*. London: Springer-Verlag.
- Shu, C.; Chew, Y. T.** (1997): Fourier expansion-based differential quadrature and its application to Helmholtz eigenvalue problems. *Communications in Numerical Methods in Engineering*, vol. 13, no. 8, pp. 643-653. DOI 10.1002/(SICI)1099-0887(199708)13:8<643::AID-CNM92>3.0.CO;2-F.
- Shu, C.; Ding, H.; Yeo, K. S.** (2003): Local radial basis function-based differential quadrature method and its application to solve two dimensional incompressible Navier-Stokes equations. *Computer Methods in Applied Mechanics and Engineering*, vol. 192, no. 7-8, pp. 941-954. DOI 10.1016/S0045-7825(02)00618-7.
- Singh, B. K.; Kumar, P.** (2018): An algorithm based on DQM with modified trigonometric cubic B-splines for solving coupled viscous Burgers' equations. *Communications in Numerical Analysis*, vol. 2018, no. 1, pp. 21-41. DOI 10.5899/2018/cna-00333.
- Tamsir, M.; Dhiman, N.; Srivastava, V. K.** (2018): Cubic trigonometric B-spline differential quadrature method for numerical treatment of Fisher's reaction-diffusion equations. *Alexandria Engineering Journal*, vol. 57, no. 3, pp. 2019-2026. DOI 10.1016/j.aej.2017.05.007.

Tang, T. (1993): A finite difference scheme for partial integro-differential equations with a weakly singular kernel. *Applied Numerical Mathematics*, vol. 11, no. 4, pp. 309-319. DOI 10.1016/0168-9274(93)90012-G.

Walz, G. (1997): Identities for trigonometric B-splines with an application to curve design. *BIT Numerical Mathematics*, vol. 37, no. 1, pp. 189-201. DOI 10.1007/BF02510180.

Wang, X. (2015): *Differential Quadrature and Differential Quadrature Based Element Methods: Theory and Applications*. Oxford: Butterworth-Heinemann, Elsevier.

Yaseen, M.; Abbas, M.; Nazir, T.; Baleanu, D. (2017): A finite difference scheme based on cubic trigonometric B-splines for a time fractional diffusion-wave equation. *Advances in Difference Equations*, vol. 2017, no. 1, pp. 291. DOI 10.1186/s13662-017-1330-z.

Zadeh, K. S. (2011): An integro-partial differential equation for modeling biofluids flow in fractured biomaterials. *Journal of Theoretical Biology*, vol. 273, no. 1, pp. 72-79. DOI 10.1016/j.jtbi.2010.12.039.

Zhang, H.; Han, X.; Yang, X. (2013): Quintic B-spline collocation method for fourth order partial integro-differential equations with a weakly singular kernel. *Applied Mathematics and Computation*, vol. 219, no. 12, pp. 6565-6575. DOI 10.1016/j.amc.2013.01.012.